APPLICATION OF MACH-ZEHNDER INTERFEROMETERS FOR ISOLATOR SHOCK TRAINS

Taishi Takeshita[1]; **Shinichiro Nakao**; **Yoshiaki Miyazato**
The University of Kitakyushu, Faculty of Environmental Engineering,
Department of Mechanical Systems Engineering,
1-1 Hibikino, Wakamatsu-ku, Kitakyushu, Fukuoka, 808-0135, Japan
e-mail: [1]y7mba011@eng.kitakyu-u.ac.jp

Abstract

A Mach-Zehnder interferometer system combined with a high-speed camera is applied for a shock train in a constant-area straight duct to clarify its unsteady characteristic in which just upstream of the shock train the freestream Mach number is 1.44, the unit Reynolds number is 4.97 × 107 m^{-1}, and the boundary layer thickness is 0.472 mm. An instantaneous two-dimensional density field in the shock train is quantitatively obtained with high spatial resolution. The present Mach-Zehnder interferometer system is found to be effective for unsteady density measurements in shock-dominated flows in a two-dimensional duct. The oscillatory characteristic of each shock in the shock train is demonstrated by power spectral analysis of the unsteady density field.

Keywords

Shock train; Supersonic flow; Unsteady flow; Mach-Zehnder interferometer; Density measurement.

Introduction

Over the past few decades, the development of dual-mode scramjet engines for realizing next-generation propulsion systems has been aggressively conducted. Dual-mode scramjet engines provide a practical solution to supersonic flight by operating under a wide range of Mach numbers. In the ramjet mode, the incoming air is compressed through shock trains known as precombustion shocks before entering the combustion chamber. To isolate the effect of flight conditions on shock trains, a nearly constant area duct referred to as an isolator is placed between the inlet and the combustor [1].

Matsuo et al.[2] have reviewed past experimental, theoretical, and numerical investigations on the subject of shock trains and showed that when a normal shock in a constant-area straight duct is strong enough to separate the boundary layer, the shock is bifurcated and one or more shocks appear downstream of the bifurcated shock. A series of repeated shocks has been called in many ways by many researchers, multiple shocks, shock systems, for example. Matsuo et al. referred to such a series of repeated shocks as a shock train in their review paper in 1999 [2]. The shock train is followed by a pressure recovery region contributed to mixed supersonic-subsonic if the duct is long enough. Therefore, the effect of the interaction extends over a great distance and the flow is decelerated from supersonic to subsonic through the whole interaction region. In this sense, the interaction region including the shock train in it is called “pseudo-shock”. However, the term “shock train” as well as “pseudo-shock” has been used in confusing way even now.

Under certain operating conditions shock trains or pseudo-shocks are widely observed in various fluid machineries such as supersonic intakes, supersonic diffusers and high-pressure

pipe lines, strongly affecting local heat transfer rates as well as aerodynamic loading. Most of the research so far has focused on time-averaged characteristics of shock trains including the length of a pseudo-shock and pressure distribution along the duct wall, the structure of shock trains by Schlieren visualization. In addition, from studies conducted mainly in the Japanese research institutions including Kyushu University, Tokyo Institute of Technology, and Muroran Institute of Technology, it is widely recognized that a shock train oscillates across its time-mean position and extreme pressure fluctuation caused by the shock train oscillation, induces vibration of the machineries or causes heavy sound noise to be emitted into the atmosphere [2]. In recent years, the physics on the behavior of an unsteady shock train has attracted much attention from researcher community engaged in the design of scramjet engines all over the world [3-9], because higher engine thrust can be achieved if a shock train is confined to the isolator of the scramjet engine and shock train oscillations have a significant effect on the unstart of the engine.

Previous research found that shock trains have two-types of unsteady motions: one is the self-excited oscillation [10, 11] associated closely with the unsteadiness induced by the interaction of a shock wave with a boundary layer, and the other is the forced-shock train oscillation [11, 12] contributed to fluctuating back-pressures. In most of the experimental studies on shock train oscillations, wall pressure measurements were performed and hence, little is investigated about the detail of unsteady characteristics inside of a shock train. Therefore, the aims of the present study are to provide reliable experimental data for validating numerical simulations of shock trains in internal gas flows and to clarify unsteady characteristics of the two-dimensional density field in a shock train in which a Mach-Zehnder interferometer system combined with a high-speed digital camera is utilized. The wedge fringe method is applied to perform the fringe shift analysis of the interferogram for density fields. The two-dimensional unsteady density field including the shock-train is for the first time elucidated by the present experiment.

1 Experimental Apparatus

Experiments were carried out in a blow down facility with a Mach-Zehnder interferometer system of High-Speed Gasdynamics Research Laboratory at the University of Kitakyushu. A schematic diagram of the experimental apparatus is shown in Figure 1. The air supplied by a compressor that pressurizes the ambient air up to 1 MPa is filtered, dried and stored in a reservoir with a total capacity of 4 m3. The high-pressure dry air from the reservoir is stagnated in a plenum chamber shown in Figure 1 and then discharged into the atmosphere through a test section. In the present experiment, the plenum pressure is controlled and maintained constant during the testing by a solenoid valve. The operating pressure ratio p_{os}/p_b of plenum pressure p_{os} to back pressure p_b was held constant at 1.7.

Figure 2 shows a schematic diagram of the test section. The test section consists of a Laval nozzle followed by a constant-area straight duct. The nozzle is designed by the method of characteristics to provide uniform and parallel flow at the nozzle exit plane and its design Mach number is 1.5. The nozzle has heights of 4.24 mm and 5 mm at the throat and exit, respectively, a constant width of 13 mm over the full length from the inlet to exit. The constant-area duct with a height of 5 mm and a width of 13 mm is connected to the exit of the supersonic nozzle. The duct has 40 static pressure measuring locations with a tap of 0.5 mm in diameter along the center line of the upper and lower walls at an equal interval of 1 mm over the range from x = 0 mm to x = 39 mm. Each static pressure tap is connected to the digital pressure sensor (Yokogawa Model MT220) with uncertainty of±50 Pa through a polyvinyl chloride tube with an inner diameter of 0.7 mm and a length of 500 mm. The dashed line in Figure 2 indicates the range of an optical window for flow visualization.

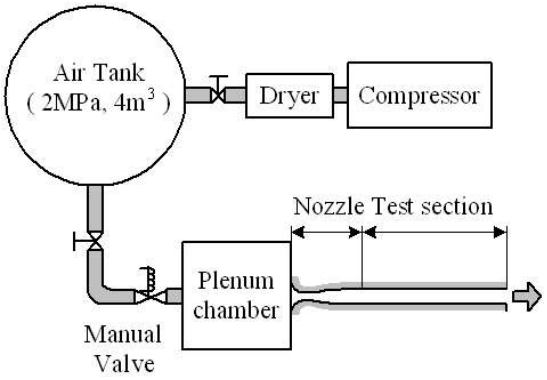

Fig. 1: Schematic diagram of experimental set up

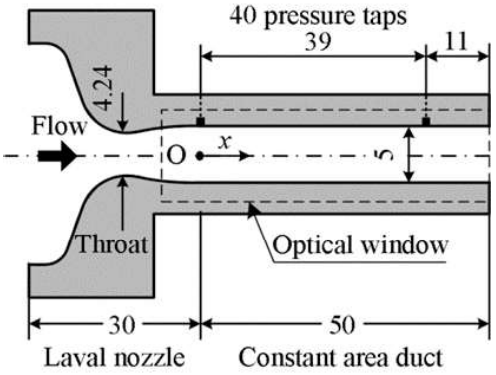

Fig. 2: Test nozzle

2 Mach-Zehnder Interferometers

As shown in Figure 3, a Mach-Zehnder interferometer system combined with a high-speed digital camera is used to measure an unsteady two-dimensional density field including a shock train and a He-Ne laser is utilized as a light source. Mach-Zehnder interferometers can estimate the unsteady features of the whole density field in the duct including the shock displacement by analyzing the fringe shift from a reference image. The wedge fringe method can measure density more minutely than the infinite fringe method by analyzing a fringe shift and it is also capable to capture density fields with high spatial resolutions, therefore, in the present work, the wedge fringe method is employed for the fringe shift analysis. Visualization of the shock train for a specified operating pressure ratio is recorded in 20,000 pictures with 2,000 frames per second. The effective spatial resolution of the present imaging system is 22 pixel/mm or 0.045 mm/pixel. Using the present Mach Zehnder system, the instantaneous position of each shock in the shock train and the corresponding frequency can be measured with high spatial and temporal resolution.

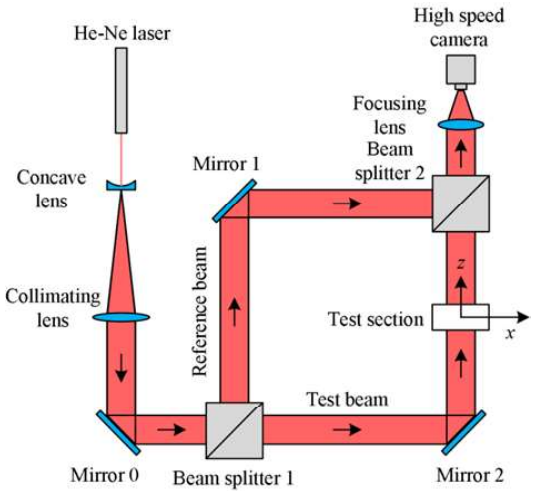

Fig. 3: Mach-Zehnder interferometer system

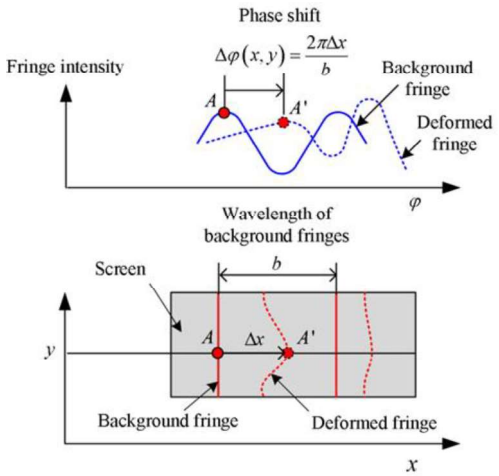

Fig. 4: Background and deformed fringe patterns

The analytical procedure for interferograms obtained from experiments is divided into two steps, which are the fringe shift analysis and density calculation from the fringe shift, see Figure 4. The former is done using the Fourier transform method, which is presented by Takeda et al. [13] and can obtain a fringe shift two-dimensionally with a high space resolution. The latter is done under the assumption that a flow field is two-dimensional. The

quantitative methodology of extracting the two-dimensional density field in the test section is described below.

The intensity profile $g(x,y)$ of the deformed fringe pattern can be given by

$$g(x,y) = g_0(x,y) + g_1(x,y)cos[k_0x + \Delta\varphi(x,y)] \quad (1)$$

with the phase shift $\Delta\varphi(x,y)$ containing the desired information on the density field in the test section where $g_0(x,y)$ and $g_1(x,y)$ represent unwanted irradiance variations arising from the nonuniform light reflection or transmission when the test beam passes through the test section, and $k_0 = 2\pi/b$. The coordinates x and y form the vertical plane, which is perpendicular to the test beam propagation direction, and the z-axis is taken as the direction in which the test beam propagates.

Eq. (1) is rewritten in the following expression

$$g(x,y) = g_0(x,y) + c(x,y)\,exp(ik_0x) + c^*(x,y)\,exp(-ik_0x) \quad (2)$$

with

$$c(x,y) = \tfrac{1}{2}g_1(x,y)\,exp[i\Delta\varphi(x,y)] \quad (3)$$

where i is the imaginary number and the asterisk * denotes a complex conjugate.

The Fourier transform of Eq. (2) with respect to x is given by

$$G(k,y) = G_0(k,y) + C(k-k_0,y) + C^*(k+k_0,y) \quad (4)$$

where the capital letters denote the Fourier transforms of the respective primitive functions and k is the spatial wave number in the x direction. Since the spatial variations of, $g_0(x,y)$, $g_1(x,y)$, $\Delta\varphi(x,y)$ and are slow compared with the spatial frequency k_0 when the interval between fringes is sufficiently small, the Fourier spectra in Eq. (4) are separated by the wave number k_0 and have the three independent peaks, as schematically shown in Figure 5 (a) [14].

We make use of either of the two spectra on the carrier, say $C(k-k_0,y)$, and translate it by k_0 on the wave number axis toward the origin to obtain $c(x,y)$, as shown in Figure 5 (b).

The unwanted background variation $G_0(k,y)$ has been filtered out in this stage by a pertinent band pass filter. We compute the inverse Fourier transform of $C(k,y)$ with respect to the k to obtain $c(x,y)$, defined by Eq. (3). Then we calculate a complex logarithm of Eq. (3) as follows:

$$\ln c(x,y) = \ln\frac{g_1(x,y)}{2} + i\Delta\varphi(x,y) \quad (5)$$

From Eq. 5, we can obtain the phase shift $\Delta\varphi(x,y)$ in the imaginary part completely separated from the unwanted amplitude variation$g_1(x,y)$ in the real part. The phase shift $\Delta\varphi(x,y)$ is related to the density field through the Gradstone-Dale formula as follows:

$$\frac{\Delta\varphi(x,y)}{2\pi} = \frac{K}{\lambda_0}\int_{-w/2}^{w/2}[\rho(x,y) - \rho_a]dz \quad (6)$$

where w = 13 mm is the span-wise length of the test section, ρ_a is the atmospheric density, λ_0 is the wavelength of a light source in vacuum, and K = 2.2587$\times 10^{-4}$ m^3/kg is the Gradstone-Dale constant. Considering the two-dimensional refractive index field, i.e., independent of the z axis, the density $\rho(x,y)$ in the flow field is expressed by

$$\rho(x,y) = \rho_a + \frac{\lambda_0}{2\pi K w}\Delta\varphi(x,y) \tag{7}$$

Since Eq. (7) shows that the phase shift at a fixed time is directly proportional to the flow density at the same time, characteristics of an unsteady flow field including a shock train can be evaluated by examining the time history of the fringe shift. An image of the flow field in the test section by the Mach-Zehnder interferometer is formed onto the CMOS sensor of a high-speed digital camera (Photron, FASTCAM SA1.1) which records a JPEG RGB image (24-bit each color) at a resolution of 1024×288 square pixels. The plane of focus is located in the front window of the test section. The RGB image is then turned into an 8-bit grayscale image by a linear transformation. Therefore, the distributions of background and deformed fringes with 256 different possible intensities can be calculated from the Mach-Zehnder images for the density-field in the test section.

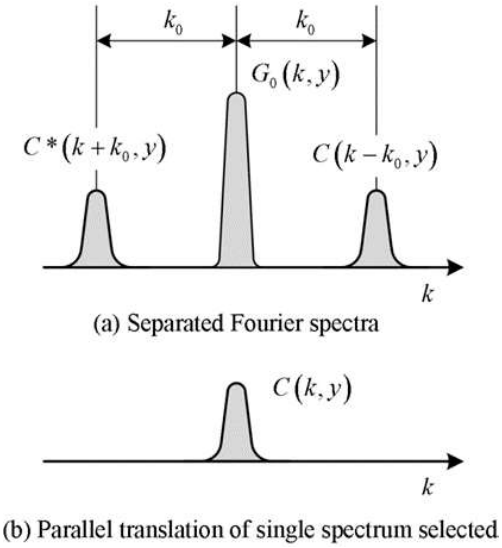

Fig. 5: *Fourier transform method fringe patterns*

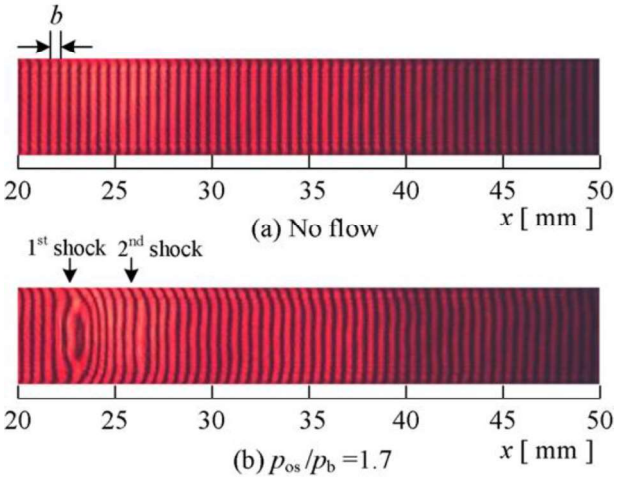

Fig. 6: *Interferograms of density field*

3 Results and Discussion

A typical interferogram before an experiment is performed (p_{os}/p_b = 1.0) is shown in Figure 6 (a) in which parallel fringes with an interval b perpendicular with respect to the duct centerline can be observed where the x is the stream-wise distance from the test section inlet. The interferograms visualized in Figure 6 (a) is called the background fringe. When the ratio of plenum to back pressures increases to p_{os}/p_b = 1.7, deformed fringes of a two-dimensional density field including a shock train with the flow from left to right are produced as shown in Figure 6 (b) in which the plenum pressure p_{os} is 172.2 kPa, the back pressure p_b is 101.3 kPa (the atmospheric pressure), and the atmospheric temperature T_b is 300.2 K.

The fringe displacements due to the interaction of a normal shock wave with a boundary layer can also be clearly seen in an area between x = 20 mm and 30 mm and fringe displacements in the stream-wise direction are almost symmetric with respect to the duct centerline. Although a shock train consisting of around two shocks can be faintly visible in the test section, we cannot obtain more information on the detailed structures of the shock train from this interferogram alone.

A typical contour plot of the two-dimensional density field including a shock train in a constant-area straight duct is presented in Figure 7 with the flow from left to right. The three

shock waves can be observed in the picture. The positions of each shock constituting the shock train are indicated in Figure 7 as the downward arrows. Just upstream of the shock train, the freestream Mach number $M_{1\infty}$ is 1.44, the unit Reynolds number Re/m is 4.97×10^7 m^{-1}, the boundary layer thickness δ_1 is 0.472 mm, and the boundary layer displacement thickness δ^*_1 is 0.189 mm. The first shock wave is bifurcated at the near the wall surface, while following two shock waves are not. The structure of the two-dimensional density field in the shock train and the downstream region is demonstrated in detail with hue spatial variations.

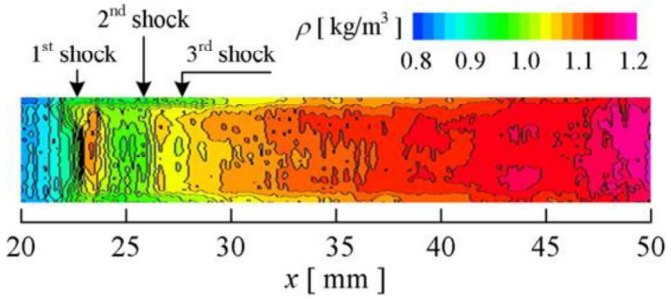

Fig. 7: *Density contour map for shock train*

The time-mean density distribution along the duct centerline in an unsteady density field including a shock train is indicated in Figure 8 where the downward arrows show the time-mean position for each shock in the shock train. It shows that a successive sudden increase in the density is due to the presence of the successive three shock waves constituting the shock-train. The steepest slope in the density is observed at the location of the first shock and the slopes of the following shocks gradually decrease in the downstream direction because the strength of the shock decreases toward the downstream. The density abruptly increases with a density spike at the location just behind of the first shock and then decreases soon before sudden increase again by the second shock and a similar density variation is repeated between the successive downstream shocks. After the shock train region, the density continues to rise gradually towards the downstream because of the mixing zone between supersonic flows near the wall surface and subsonic flows after the shock train [1] and it finally becomes to be equal to the atmospheric density at the nozzle exit.

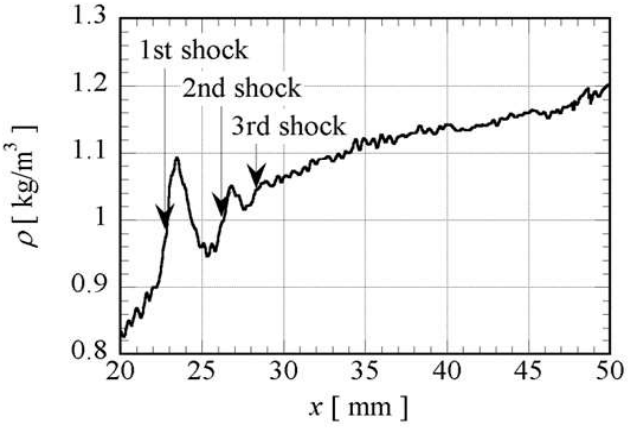

Fig. 8: *Centerline density profile in shock train*

The power spectral density distributions of the density fluctuation responsible for the oscillation of each shock in the shock train are given in Figure 9 where the density time histories are captured at the time-mean position of each shock at the duct centerline. The first shock wave oscillates at a dominant frequency of around 10 Hz and the second and third

shocks also show almost the same dominant frequency. These dominant frequencies obtained from the density fluctuations are of almost the same order of magnitude as those from wall pressure measurements in a past research [1].

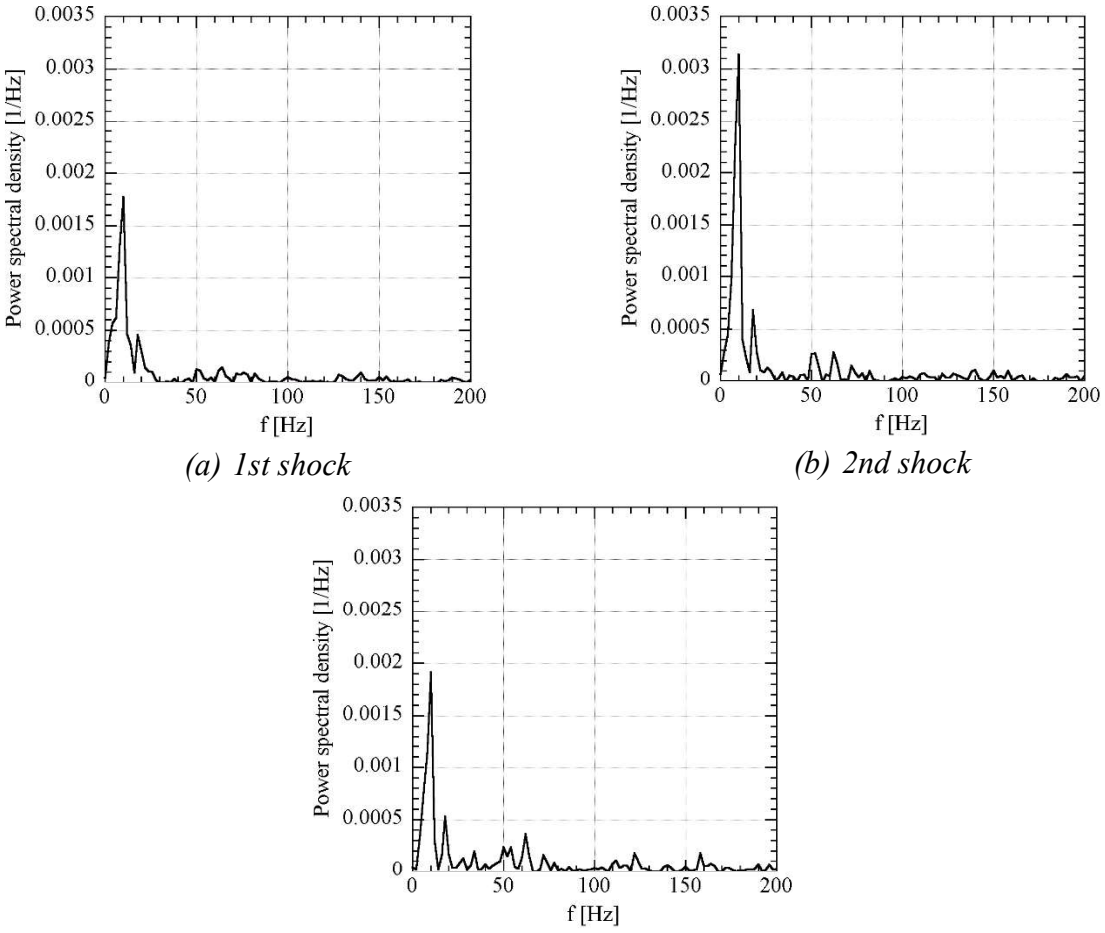

(a) 1st shock *(b) 2nd shock*

(c) 3rd shock

Fig. 9: *Power spectral density for each shock in shock train*

Conclusions

The Mach-Zehnder interferometer is effective in studying quantitatively the density fields in supersonic flows at high precision and high spatial resolution. However, there has been nopractical application of the Mach-Zehnder interferometer for shock trains. The present study quantitatively observed the two-dimensional unsteady density field including a shock train using a high-speed Mach-Zehnder system. The unsteady characteristic of each shock in the shock train was shown by the power spectral density representation. As a result, it is found that the present high-speed Mach-Zehnder system is an effective tool to investigate quantitatively the dynamics of the interaction of a shock wave with a turbulent boundary layer in a two-dimensional confined duct.

This research is an extension of the previous experimental study [15] in which the rainbow Schlieren deflectometry was applied for measurements of the density field in a shock-train and time-mean flow characteristics of the shock train were quantitatively captured. The present results from the Mach-Zehnder interferometer will be compared with those from the rainbow Schlieren deflectometry in the near future.

Acknowledgment

The authors would like to gratefully acknowledge the assistance of graduate students Yusuke Awata and Yuki Sakamoto of the University of Kitakyushu for their invaluable support to the experimental work and exceptional skills in the fabrication of the facility.

Nomenclature

i	imaginary number
g_0	background intensity
g_1	amplitude of the intensity distribution of fringes
k_0	wave number
φ	fringe shift distribution, rad
x	stream-wise coordinate from the throat, mm
y	vertical coordinate on lower wall, mm
λ_0	wave length of a light source in vacuum, nm
K	Gladstone-Dale constant, m^3/kg
w	span-wise width of duct, mm
M	Mach number
R	gas constant, J/kg·K
Re/m	unit Reynolds number, 1/m
T	temperature, K
δ^*	boundary layer displacement thickness, mm
δ	boundary layer thickness, mm
ρ	density, kg/m^3
ρ_a	the atmospheric density, kg/m^3

Subscripts

b	value at surrounding air
os	total or stagnation state
1	just upstream of shock train

Literature

[1] MATUO, K.; MIYAZATO, Y.; KIM, H.-D.: Shock train and pseudo-shock phenomena in internal gas flows. *Progress in Aerospace Sciences*. 1999, Vol. 35, Issue 1, pp. 33–100. DOI: 10.1016/S0376-0421(98)00011-6

[2] GNANI, F.; ZARE-BEHTASH, H.; KONTIS, K.: Pseudo-shock waves and their interactions in high-speed intakes. *Progress in Aerospace Sciences*. 2016, Vol. 82, pp. 36–56. DOI: 10.1016/j.paerosci.2016.02.001

[3] LEE, H. J.; LEE, B. J.; KIM, S. D.; JEUNG, I.-S.: Investigation of the pseudo-shock wave in a two-dimensional supersonic inlet. *Journal of Visualization*. 2010, Vol. 13, Issue 1, pp. 25–32. DOI: 10.1007/s12650-009-0008-3

[4] QIN, B.; CHANG, J.; JIAO, X.; BAO, W.; YU, D.: Numerical investigation of the impact of asymmetric fuel injection on shock train characteristics. *Acta Astronautica*. 2014, Vol. 105, Issue 1, pp. 66–74. DOI: 10.1016/j.actaastro.2014.08.025

[5] XU, K.; CHANG, J.; ZHOU, W.; YU, D.: Mechanism of shock train rapid motion induced by variation of attack angle. *Acta Astronautica*. 2017, Vol. 140, pp. 18–26. DOI: 10.1016/j.actaastro.2017.08.009

[6] LI, N.; CHANG, J.; YU, D.; BAO, W.; SONG, Y.: Mathematical Model of Shock-Train Path with Complex Background Waves. *Journal of Propulsion and Power*. Vol. 33, Issue 2, pp. 468–478. DOI: 10.2514/1.B36234

[7] DENG, R.; JIN, Y.; KIM, H. D.: Numerical simulation of the unstart process of dual-mode scramjet. *International Journal of Heat and Mass Transfer*. 2017, Vol. 105, pp. 394–400. DOI: 10.1016/j.ijheatmasstransfer.2016.10.004

[8] SU, W.-Y.; CHEN, Y.; ZHANG, F.-R.; TANG, P.-P.: Control of pseudo-shock oscillation in scramjet inlet-isolator using periodical excitation. *Acta Astronautica*. 2018, Vol. 143, pp. 147–154. DOI: 10.1016/j.actaastro.2017.10.040

[9] JIAO, X.; CHANG, J.; WANG, Z.; YU, D.: Periodic forcing of a shock train in a scramjet inlet-isolator at overspeed condition. *Acta Astronautica*. 2018, Vol. 143, pp. 244–254. DOI: 10.1016/j.actaastro.2017.12.005

[10] XIONG, B.; WANG, Z.-G.; FAN, X.-Q.; WANG, Y.: Experimental study on the flow separation and self-excited oscillation phenomenon in a rectangular duct. *Acta Astronautica*. 2017, Vol. 133, pp. 158–165. DOI: 10.1016/j.actaastro.2017.01.009

[11] XIONG, B.; FAN, X.-Q.; WANG, Y.; TAO, Y.: Experimental Study on Self-Excited and Forced Oscillations of an Oblique Shock Train. *Journal of Spacecraft and Rockets*. 2018, Vol. 55, Issue 3, pp. 640–647. DOI: 10.2514/1.A33973

[12] XIONG, B.; WANG, Z.-G.; FAN, X.-Q.; WANG, Y.: Response of Shock Train to High-Frequency Fluctuating Backpressure in an Isolator. *Journal of Propulsion and Power*. 2017, Vol. 33, Issue 6, pp. 1–9. DOI: 10.2514/1.B36291

[13] TAKEDA, M.; INA, H.; KOBAYASHI, S.: Fourier-transform method of fringe-pattern analysis for computer-based topography and interferometry. *Journal of the Optical Society of America*. 1982, Vol. 72, Issue 1, pp. 156–160. DOI: 10.1364/JOSA.72.000156

[14] YAGI, S.; INOUE, S.; NAKAO, S.; ONO, D.; MIYAZATO, Y.: Optical Measurements of Shock Waves in Critical Nozzles at Low Reynolds Numbers. *Journal of Flow Control, Measurement & Visualization*. 2017, Vol. 5, Issue 2, pp. 36–50. DOI: 10.4236/jfcmv.2017.52003

[15] TAKESHITA, T.; TAKANO, H.; ONO, D.; NAKAO, S.; MIYAZATO, Y.: Rainbow Schlieren visualization of shock trains in rectangular ducts. In: *Proceedings of the 23rd International Symposium on Air Breathing Engines (ISABE 2017)*. [online]. 2017. Available from WWW: https://www.isabe.org/

POUŽITÍ MACH-ZEHNDEROVA INTERFEROMETRU V ŘETĚZCI RÁZU VLN („SHOCK TRAINS“) IZOLÁTORU

Systém Mach-Zehnderova interferometru kombinovaný s vysokorychlostní kamerou se aplikuje na řetězec rázu („shock train“) konstantním přímém kanálu pro vyjasnění jeho nestabilní charakteristiky, kde je Machovo číslo 1,44, Reynoldsovo číslo je 4,97 x 107 m^{-1} a tloušťka hraniční vrstvy je 0,472 mm. Okamžitého dvojrozměrného hustotního pole v řetězci rázu je kvantitativně dosaženo s vysokým prostorovým rozlišením. Současný Mach-Zehnderův interferometrický systém se jeví jako účinný pro měření nestálé hustoty v rázově dominantních proudech v dvojrozměrném kanálu. Oscilační charakteristika každého rázu v rázovém řetězci je demonstrována výkonovou spektrální analýzou pole nestálé hustoty.

DIE VERWENDUNG DES MACH-ZEHNDER-INFEROMETERS IN DER KETTE VON SCHOCKWELLEN („SHOCK TRAINS“) DES ISOLATORS

Das System des Mach-Zehnder-Interferometers ist mit einer Hochgeschwindigkeitskamera kombiniert und findet Anwendung für die Kette von Schockwellen („shock trains“) in einem konstanten direkten Kanal zur Klärung seiner instabilen Charakteristik, wobei die Machzahl 1,44, die Reynoldszahl 4,97 x 107 m^{-1} und die Dicke der Grenzschicht 0,472 beträgt. Ein sofortiges zweidimensionales Dichtigkeitsfeld in der Kette der Stoßwellen wird quantitativ mit einer hohen Raumunterscheidung erreicht. Das gegenwärtige Mach-Zehnder-interferometrische System erweist sich als wirksam für die Messung unbeständiger Dichte in stoßdominanten Strömungen im zweidimensionalen Kanal. Die Oszillationscharakteristik eines jeden Stoßes in der Stoßkette wird durch eine Leistungsspektralanalyse des Feldes der unbeständigen Dichte demonstriert.

ZASTOSOWANIE INTERFEROMETRU MACHA-ZEHNDERA W ŁAŃCUCHU FAL UDERZENIOWYCH („SCHOCK TRAINS”) IZOLATORA

Zestaw interferometru Macha-Zehndera połączony z szybką kamerą zastosowany został do łańcucha uderzeń („shock train”) w stałym prostym tunelu w celu wyjaśnienia jego niestabilnej cechy, przy czym liczba Macha wynosi 1,44, liczba Reynoldsa wynosi 4,97 x 107 m^{-1} a grubość warstwy granicznej to 0,472 mm. Pod względem jakościowym, natychmiastowe dwuwymiarowe pole gęstości powstaje w łańcuchu uderzeń z dużą rozdzielczością przestrzenną. Obecny zestaw interferometru Macha-Zehndera wydaje się skuteczny w przypadku pomiarów niestabilnej gęstości w zdominowanych przez wstrząsy przepływach w dwuwymiarowym tunelu. Oscylacyjna charakterystyka każdego wstrząsu w łańcuchu uderzeń prezentowana jest poprzez analizę spektralną pola niestabilnej gęstości.